

**"A Cochlear Nucleus Auditory
Prosthesis based on microstimulation"**

Contract No. **No. NO1-DC-4-0005**
Progress Report #9

HUNTINGTON MEDICAL RESEARCH INSTITUTES
NEURAL ENGINEERING LABORATORY
734 Fairmount Avenue
Pasadena, California 91105

D.B. McCreery, PhD
Martin Han, PhD
Victor Pikov, PhD

HOUSE EAR INSTITUTE
2100 WEST THIRD STREET
Los Angeles, California 90057

R.V. Shannon, PhD
Steve Otto, MS

I: work at Huntington Medical Research Institutes

I.1 Progress in the fabrication of multisite silicon probes

At HMRI, we have been developing processes for fabricating silicon-substrate probes. The HMRI silicon probes provide several advantages for long-term stimulation and recording of neuronal activity (1) mechanically-strong and thickness-controllable probe shafts, (2) multiple recording and stimulation sites on single or multiple shaft(s), and (3) three-dimensional (conformal) insulation.

We have been using deep reactive ion etching (DRIE) technology to shape the silicon shafts, and have successfully fabricated probes 50 to 120 μm in thickness (Figure C11), with excellent control and uniformity of thicknesses across 4-inch silicon wafers. By repeating cycles of polymer deposition and reactive ion etching (Bosch, 1994), the DRIE technology enables fabrication of well-defined vertical wall features (Figure 1A). The thicknesses of the probe shafts can be controlled precisely between a few microns to several hundreds microns, by using either silicon-on-insulator wafers or by controlling etching depths on plain silicon wafers, as shown in Figure 1A. After removal from the wafer, the probes are coated on all surfaces with Parylene-C, which then is ablated from the electrodes sites and bonding pads using our eximer laser (Figures 1C-E).

We have adapted EIC Laboratories' procedure for electroplating iridium oxide onto the electrode sites (Meyer et al, 2001). A plated site is shown in figure 1E. This treatment greatly increases the electrodes' charge capacity during controlled-current pulsing, and by reducing electrical impedance, reduces Johnson noise during recording of neuronal activity. Each of 4 sites on a test probe were able to inject 400 $\mu\text{C}/\text{cm}^2$ of charge into phosphate-buffered saline, with a total potential excursion $< \pm 0.9$ V.

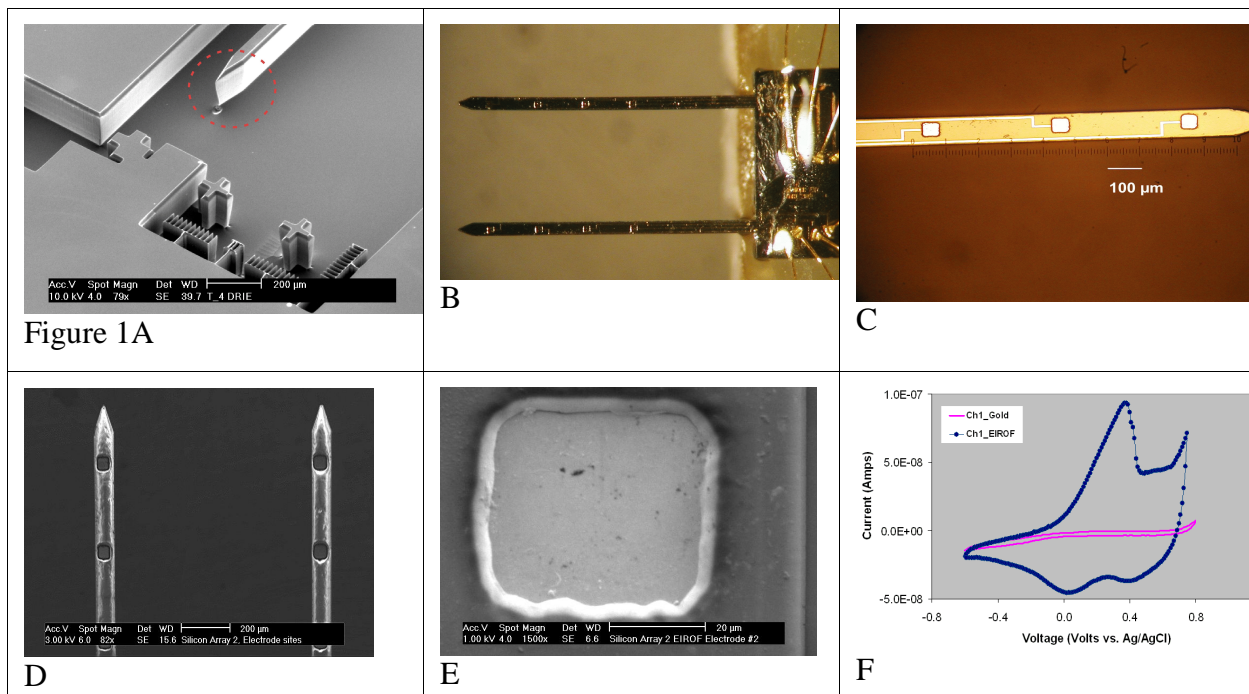


Figure 1 shows silicon probes fabricated by HMRI. Figure 1A shows scanning electron microscopic (SEM) image of various designs and features fabricated using DRIE, exhibiting excellent uniformity of thicknesses across 4-inch diameter silicon wafers. Figure 1B shows a 2-shank, 100 μm thick stimulating probe for the feline cochlear nucleus, mounted for soak-testing. Figure 1C is a light-micrograph of one of the probe shafts shown in B, showing 3 of the electrode sites. Figure 1D is a SEM of the shafts, showing 4 of the electrode sites opened in the 3 μm conformal Parylene-C coating by the eximer laser. A SEM of one of the stimulating sites plated with electrodeposited iridium oxide film (EIROF) is shown in figure 1E. .

Figure 1F is a cyclic voltammograms of the stimulating site before (red) and after (blue) being electroplated with EIROF, illustrating a large increase in charge capacity. Scan rate was 50 mV/sec.

The silicon-based probes are fabricated in the Micromaching Laboratory, at the California Institute of Technology. The main fabrication steps are illustrated in figure 2. (a) Layers of 0.3 μm -thick silicon nitride (SiN_x) and 0.2 μm -thick SiO_2 dielectric coatings are deposited by plasma-enhanced chemical vapor deposition (PECVD) onto the SiO_2 -grown SOI wafers.

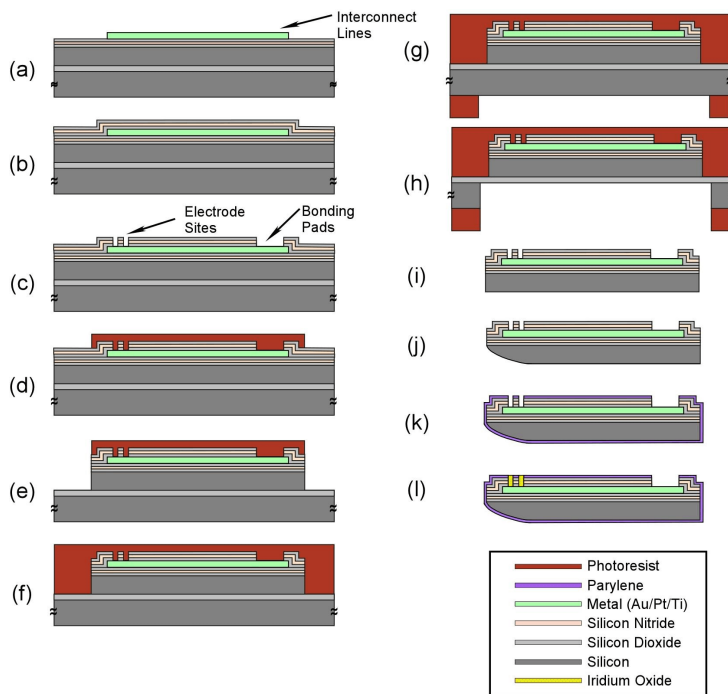


Figure 2

(a) Layers of 0.3 μm -thick silicon nitride (SiN_x) and 0.2 μm -thick SiO_2 dielectric coatings are deposited by plasma-enhanced chemical vapor deposition (PECVD) onto the SiO_2 -grown SOI wafers. (b) A patterning of bilayer photoresists (AZ 1518 and Lift-off-Resist) with undercuts is photolithographically achieved to allow for the lift-off of evaporated 0.03 μm -thick titanium, 0.03 μm platinum and 0.2 μm gold films, defining the transmission lines and the bases of active electrodes. (c) Deposition of insulation layers SiO_2 - SiN_x - SiO_2 by PECVD is performed. (d) Anisotropic reactive ion etching ($\text{CF}_4 + \text{O}_2$ plasma) is subsequently performed to etch the SiO_2 - SiN_x - SiO_2 triple "sandwich" dielectric coatings, thereby opening electrodes and bonding pad sites by photolithography process and reactive ion etching (RIE). (e) A thick photoresist layer (AZ4400) is spun and is patterned to shape an overall probe structure, (f) RIE of the dielectric layers, followed by DRIE of the top silicon bulk, is performed until the buried SiO_2 -etch-stop layer is reached. (g) After stripping the existing photoresist layer, another layer of thick photoresist (AZ4620) is spun to protect the top and sides of the probe. (h) Back-side photolithography with a thick PR is done. (h) Back-side DRIE is performed. (i) Wet-etching of the SiO_2 etch-stop layer with buffered hydrofluoric acid, followed by PR-stripping, is performed thereby releasing individual probes. (j) The tips are mechanically ground to bevel (k) The entire probes is coated with a 3 μm conformal insulating layer of Parylene-C, followed by opening the electrode sites and bonding pads with eximer laser, following by cleaning with oxygen plasma. Finally, (l) iridium oxide is electrodeposited onto the electrode sites.

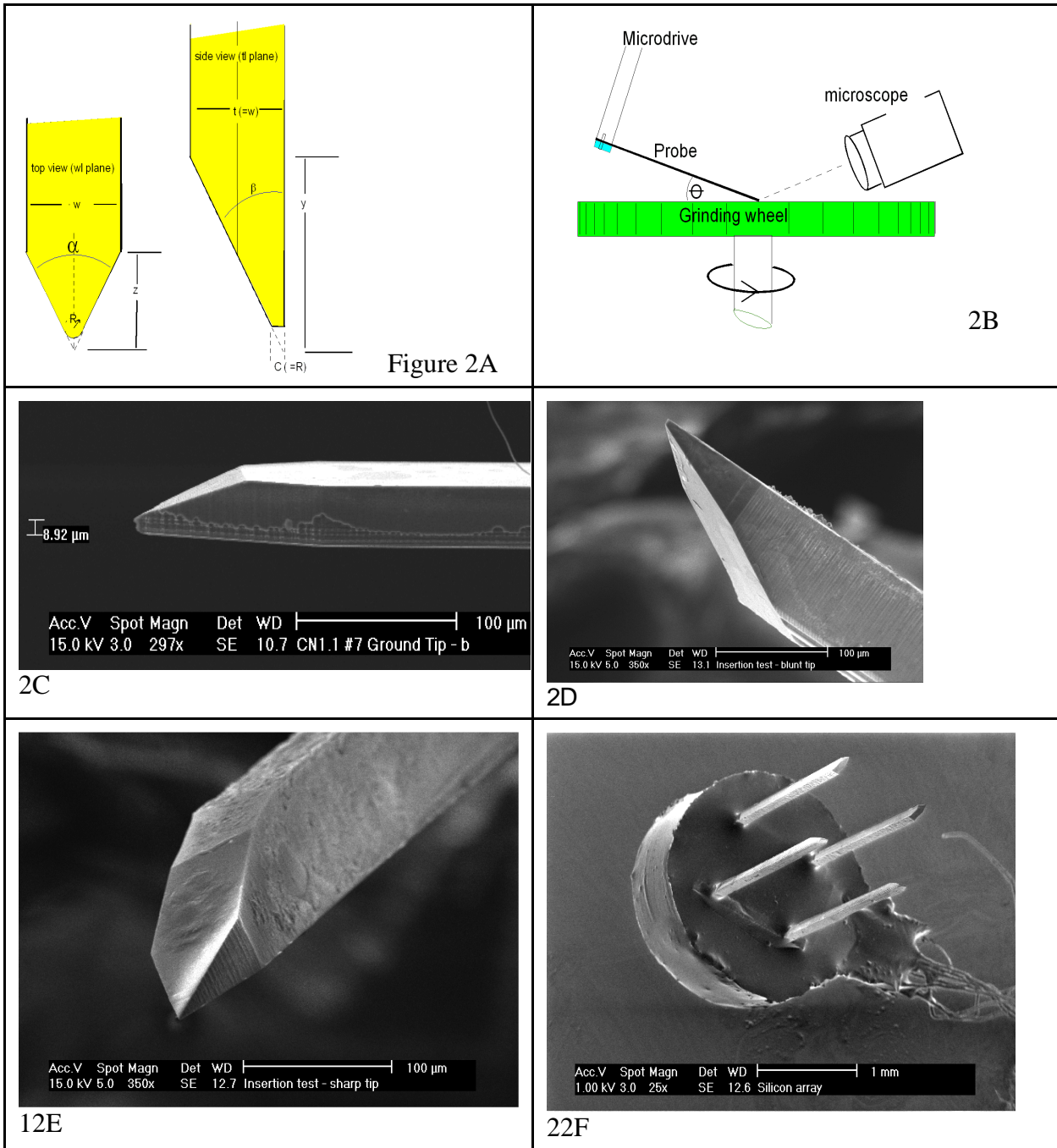


Figure 2A

2B

2C

2D

12E

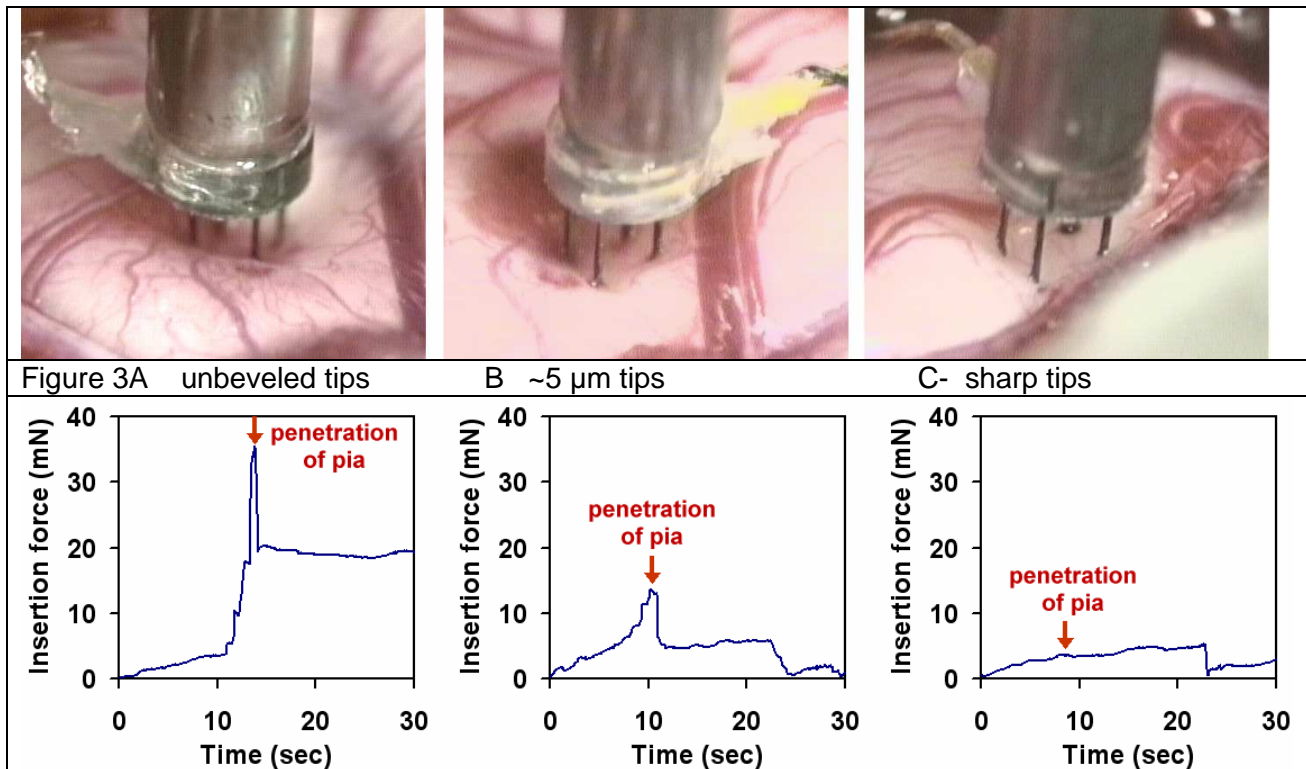
22F

DRIE yields mechanically sturdy probes whose width and thickness can be scaled to best accommodate various probe lengths and numbers of sites. thus long (2.g., 4 mm) probes do not flex as they attempt to penetrate through the pia, and they do exhibit the slight curvature in the plane normal to the features, as is characteristic of probes produced by the deep boron etch process. The ability to produce shafts of any thickness is especially valuable when long probes are required, such as will be necessary when recording along the tonotopic axis of the cats' inferior colliculus, or when penetrating a thickened pia mater, as when multisite probes are implanted in the human cochlear nucleus or inferior colliculus.

However, one limitation of DRIE is that the wafer is etched in one dimension (Figure 1A), so the probes have chisel-like tips. In order to penetrate through the pia mater and then pass through the brain parenchyma with minimal disruption and damage, the tips must be beveled in order to remove or reduce the chisel edge. The parameters of the bevel, β and C , are shown in profile in figure 2A and

are formed by post-wafer grinding. For that procedure, the probe is mounted on a spring-loaded fixture attached to a microdrive and thereby brought into contact with a rotating grinding wheel charged with 0.8 μm diamond particles. The operation is observed through a microscope so that the width of the C-segment can be controlled (Figure 2B). The operation requires a few minutes per probe and is quite reproducible. Figures 2C,D & E show scanning electron micrographs of probes with various C-values, from approximately 10 μm (2C) to a sharply pointed tip (2E). All of the tip regions have cutting edges above the actual tip, to facilitate penetration of the pia. Figure 2F is an SEM of an array of 2 probes and 4 shanks with beveled tips, that we use to compare the ability of tips with various C-values to penetrate through the pia of the feline cerebral cortex.

In order to evaluate the performance of silicon probes with different tip geometries, we used a micromanipulator to insert arrays similar to figure 2F through the pia mater covering the cerebral cortex of an anesthetized cat (Figure 3). We evaluated three types of arrays: those with unbeveled tips, those beveled to a small ($\sim 5 \mu\text{m}$) chisel-edge at the tip (“blunt” tips, Figure 2D) and with sharply pointed tips, with the bevel extending up to the feature plane (“sharp” tips, Figure 2E).



We monitored the force exerted by the manipulator on the probe using a force transducer (Figure 3 lower row) and monitored the amount of dimpling of the pia using video microscopy (upper row). The force measurements indicate that an array with unbeveled tips required 35 mN or more to penetrate the pia of the cerebral cortex, and depressed the pia and the brain by about 2 mm before penetrating the pia (Figure 3A). On 2 of 6 attempts, the unbeveled tips did not penetrate the pia, even with a force of 100+ mN. Arrays with beveled tips penetrated into the brain after much less dimpling of the pia and depression of the brain (Figure 3B,C). The arrays with “blunt” ground tips ($\sim 5 \mu\text{m}$ chisel edge) required a force of approximately 13 mN to penetrate the pia (Figure 3B), and an array with sharp ground tips (no chisel edge) required 3.5 mN (Figure 3C). The insertion tests were conducted 6 times for each array type. The results indicate that the probes with the double cutting-type tip regions can easily penetrate the thick pia matter over the medial part of the cat’s cerebral hemispheres, and also demonstrates the value of probes with very sharp tips. However, it is not certain that these very sharp tips will inflict the least amount of injury during their subsequent passage through the underlying brain parenchyma.

Introduction of these probes into our cochlear nucleus project has been delayed due to an unrelated injury to one of our technicians. In the next quarter, we expect to begin using a 16-site version for recording of neuronal activity in the inferior colliculus, and to begin implanting arrays similar

to figure 2F into the cats' ventral cochlear nucleus.

I.2 Comparison of micro-and macrostimulating electrodes in the cat cochlear nucleus.

Part of the work scope of our contract call for us to objectively compare the ability of penetrating microstimulating electrodes and surface macroelectrodes to selective activate the tonotopic organization of the ventral cochlear nucleus. We have begun these studies using stimulating arrays similar to our cat cochlear nucleus array with 16 stimulating sites on 4-shanks, but with 2 macroelectrodes on the under surface. These have a geometric area of approximately 0.4 mm^2 , and are set between the silicon shanks which in figure 4 are oriented towards the camera. The array superstructure is implanted on the dorsolateral surface of the cochlear nucleus with one macroelectrode dorsal and medial and the second ventral and lateral, so that the medial macroelectrode will access the high acoustic frequencies and the lateral electrode will access low frequencies. The silicon shanks penetrate into the ventral cochlear nucleus. In our cat model, the spread of neuronal activity along the tonotopic gradient of the ventral cochlear nucleus is quantified as the spread of activity along the dorsolateral-ventromedial axis of the central nucleus of the inferior colliculus, using the techniques described in our pervious quarterly reports. Selectivity of the stimulation then was quantified for each electrode and for each stimulus amplitude, as the ratio of the maxima of the neuronal activity induced in the ICC, to the span of activity in the ICC to the.

Two experiments have been completed. Data analysis from the first experiments is complete and analysis of the data from the second is underway. In the cat for which analysis is complete, the selectivity of the microelectrodes was markedly greater than that of the surface electrodes for the portion of the tonotopic gradient that encodes low acoustic frequencies, but was similar for high frequencies. This work is continuing and will be reported in detail in the next quarterly report.

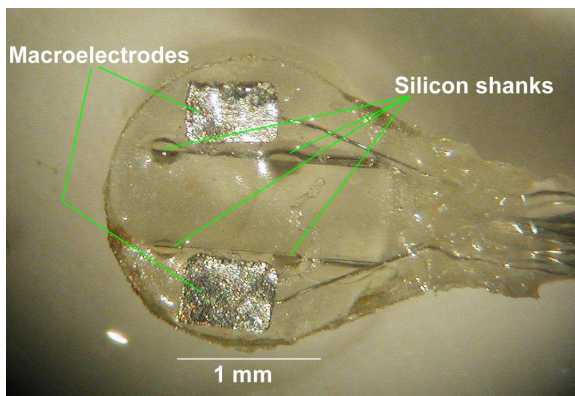


Figure 4

Publication:

D. McCreery, Lossinsky A, and Pikov V. Performance of multisite silicon microprobes implanted chronically in the ventral cochlear nucleus of the cat. *Accepted for publication in IEEE Trans Biomed Engr.*

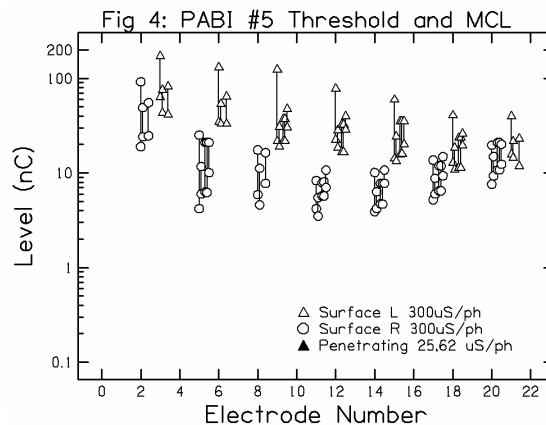
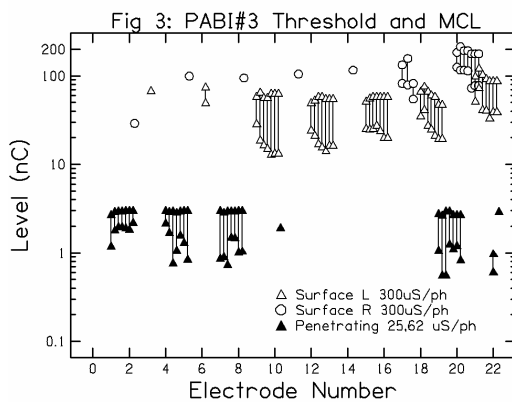
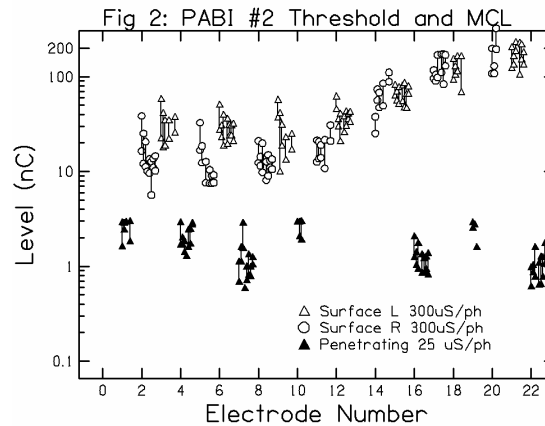
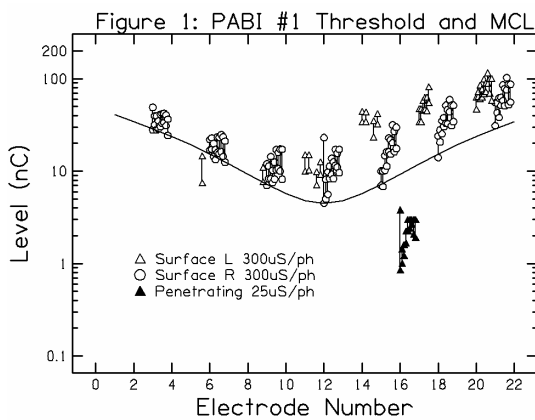
II. Work completed at the House Ear Institutes

Overview

Patients with the penetrating auditory brainstem implant “PABI patients” 1, 2, 3, 5, 6, and 7 were seen in this quarter. PABI patients 1, 2, 3, and 5 were seen as part of the routine follow-up protocol. PABI patients 2, 6 and 7 were seen in a special testing session to determine the causes and solution to the problem of undesirable activation of the spinal root of the trigeminal nerve, as reported in the previous quarterly report. In this report we will present the results of standard tests of threshold and speech recognition on all patients, results of new psychophysical tests, and a special report on trigeminal nerve activation on PABI patients 6 and 7.

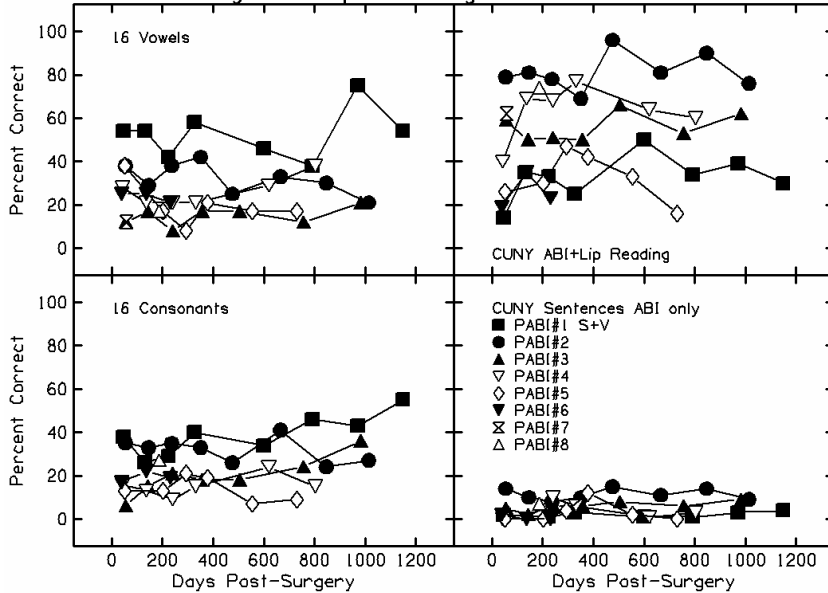
Threshold and Dynamic Range

Figures 1-4 present threshold and dynamic range measures from PABI patients 1, 2, 3 and 5, respectively.



Each cluster of data points represent repeated measures over time, with the time interval between data points typically 3 months. Each pair of two points connected by vertical lines represent the threshold and maximum comfortable loudness levels measured using the standard clinical method. Surface electrodes are shown as open symbols and penetrating electrodes are shown as filled symbols. In most cases the repeated measures show good stability over time. In general, penetrating electrodes produced thresholds that were below 1 nC and the upper range on penetrating electrodes was typically limited by the charge limit (3 nC for PABI generation 1, 8 nC for PABI generation 2 penetrating electrodes with larger exposed surface area).

Fig 5: ABI Speech Recognition over Time

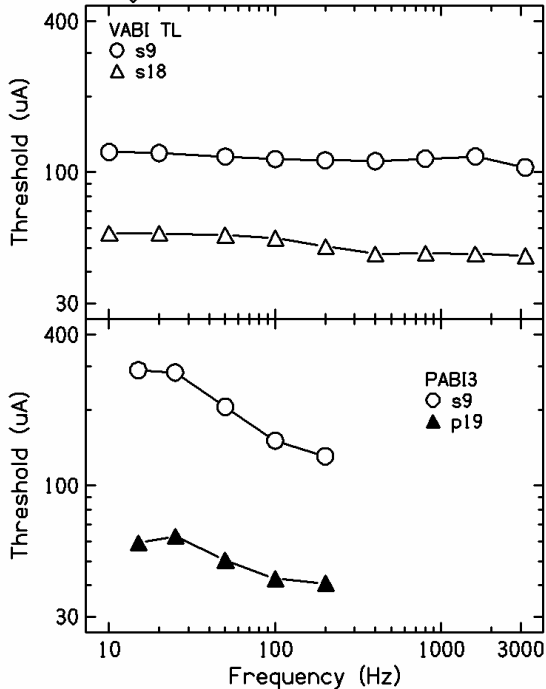


Speech Recognition

Figure 5 shows results from selected speech recognition measures over time for all PABI patients. Filled symbols present results from PABI patients who use penetrating electrodes in their speech processor maps and open symbols show results from patients who cannot use penetrating electrodes in their maps. The two left panels show results from vowel (upper) and consonant (lower) phoneme recognition tests. Chance performance is 12.5% correct on the vowel test and 6.25% correct

for the consonant test. There was no clear trend for improved performance over time. Patients using penetrating electrodes do appear to recognize consonants at a slightly higher level than patients without penetrating electrodes. The right panels show recognition of simple sentences (CUNY) either using only the sound from the PABI (lower panel) or in combination with lip-reading (upper panel). Note that the best performance of a PABI patient is about 15% open set recognition of sentences with sound from the device alone. This patient (PABI#2) is also an excellent lip-reader and in combination with lip-reading she is able to obtain 80% correct on sentence recognition. However, most PABI patients show no improvement in performance over time - there is no indication of long-term learning even over three years.

Figure 6: Threshold vs Pulse Rate



Threshold as a Function of Pulse Rate

One potential difference between cochlear implants, brainstem implant surface electrodes and penetrating brainstem electrodes is in terms of the basic perceptual consequences related to the specific types of neurons stimulated. One potential difference is in terms of the integration time of the nerve membrane. As an indication of neural/perceptual integration time we measured thresholds as a function of the stimulation rate. Figure 6 compares threshold measures as a function of stimulation rate in two patients: one PABI patient and one non-NF2 ABI patient. For each patient we selected two electrodes: one with a high threshold level and one with a low threshold level. In the PABI patient the low-threshold electrode was a penetrating electrode (p19). Note that the thresholds are almost unaffected by rate in the non-NF2 ABI patient - both curves are almost flat as a function of pulse rate. This result is similar to that obtained previously in ABI listeners (Shannon, 1989) and is different from the pattern observed in CI listeners (Shannon, 1985).

Threshold functions for CI listeners are flat as a function of stimulation rate and then drop at 3-4 dB/octave at stimulation rates above about 250 pps. This pattern can be modeled as a

rectifying nonlinearity followed by a simple integration mechanism with a 2 ms time constant (Shannon, 1989b). The flat curves observed in most ABI listeners (top panel in Figure 6) suggest little or no integration out to inter-pulse times of less than 0.3 ms. However, the curves in the lower panel obtained from PABI#3 show significant lowering of threshold as a function of stimulation rate, suggesting considerable integration with a relatively long integration time constant (more than 30 ms). A similar time constant was observed for both the surface electrode and penetrating electrode. It is not clear at this time why there would be such a large difference across ABI patients. The difference observed in Figure 6 is not likely to be due to the penetrating electrode device, because the difference in threshold function was also observed on the surface electrode in this patient. Note that patients ABI#8 and PABI#3 were both NF2 patients while VABI TL was an ABI patient with severe ossification of the cochlea and modioulus. VABI TL was able to understand more than 90% correct on sentence material with only the sound from the ABI, whereas both NF2 listeners could understand less than 10% of words in sentences with only the sound from the ABI/PABI.

Threshold as a Function of Pulse Phase Duration

Another perceptual measure that might indicate the time constant of stimulated neurons is threshold as a function of pulse phase duration. Biphasic, charge-balanced pulses were always used to achieve zero net charge delivered and the anodic phase was presented first. The two phases of each biphasic pulse are separated by a 45 μ s interval. Pulses were presented at a low rate, either 15 or 20 pps to minimize any effects that would carry over

across pulses.

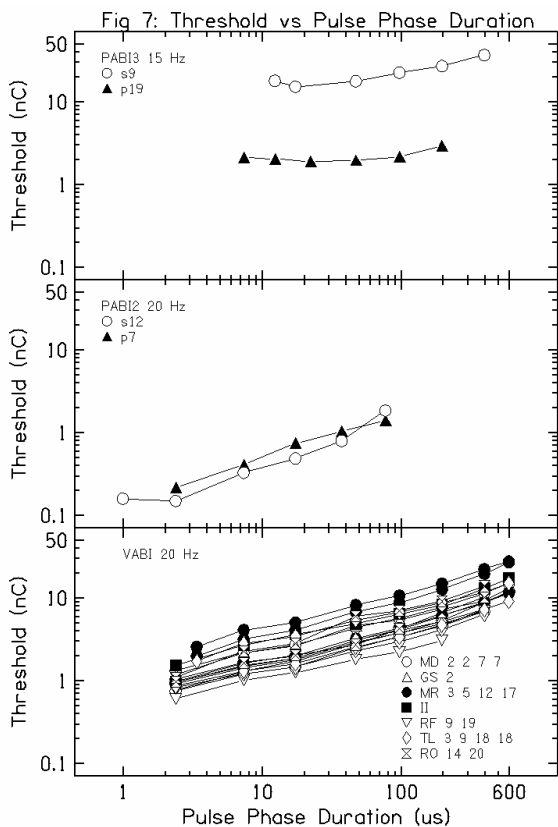
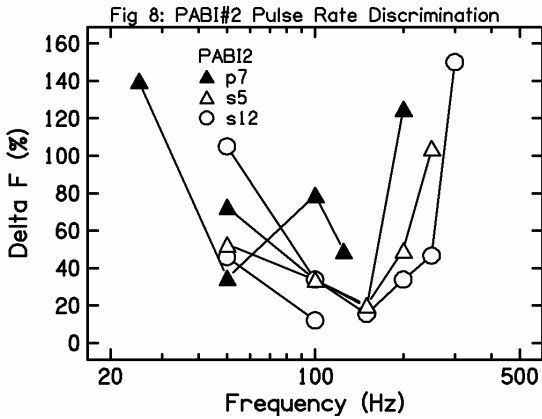


Figure 7 presents the results from two PABI patients (middle and top panel) compared to data from 6 ABI non-NF2 patients from Verona who are all excellent at speech recognition (>50% correct on sentences). The numbers on the lower panel indicate the electrode numbers tested (all surface ABI electrodes with some repeated measures). In the upper two panels the open symbols indicate surface electrodes and filled symbols indicate penetrating electrodes. Note that the functions are approximately linear on log-log axes, indicating that the relation between charge and pulse duration is a power function. If threshold were determined by a constant amount of charge then these functions would all be horizontal lines, indicating constant charge as a function of pulse phase duration. However, it is clear that the functions are not flat and that the amount of charge required for threshold stimulation increases as pulse duration increases, i.e. short pulses are most efficient. Slopes of curves are about 0.5 for Verona non-NF2 patients and for PABI2, but shallower for PABI3. Similar results from cochlear implants (Zeng, Galvin and Zhang, 1998) found a slope of about 0.3 for threshold and 0.6 for MCL. A slope of 0.5 indicates that the pulse amplitude trades off with the square root of pulse phase duration to achieve equal sensation magnitude. Note that for PABI#2 (middle panel) the slope for the penetrating PABI electrode was similar to the slope for the surface electrode. However for PABI#3 the curve for the penetrating electrode was nearly flat, indicating constant amount of charge at threshold regardless of pulse phase duration.

Pulse Rate Discrimination

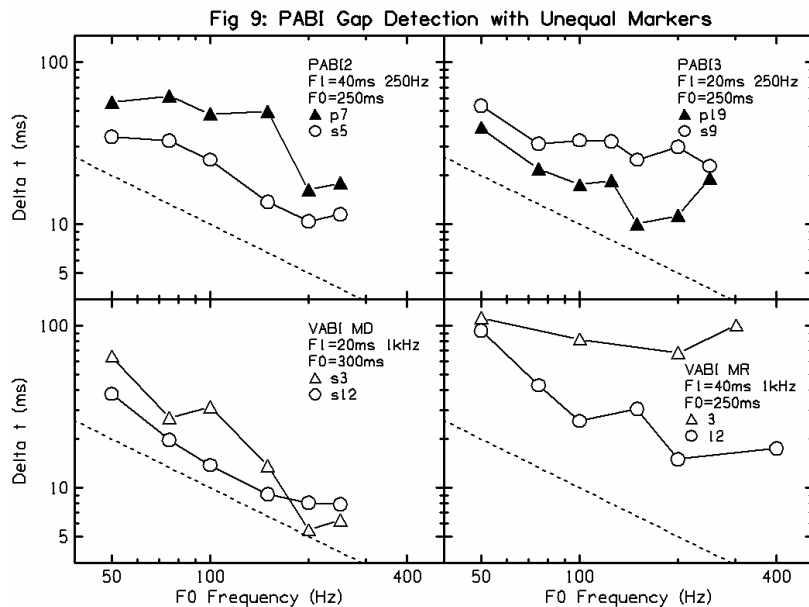
Additional measures were made during the last quarter of pulse rate discrimination in PABI#2. The ability to discriminate pulse rates is theoretically useful for separating male and female talkers, for discriminating questions from statements, and for detecting vocal emphasis and emotion. Cochlear implant listeners can typically detect a change of 7-10% in pulse rate up to rates of about 300 Hz. For higher pulse rates most CI listeners cannot detect changes in rate - even changes of one octave or more. Measures of pulse rate discrimination were made in ABI and PABI listeners for comparison. Figure 8



presents recent measurements of pulse rate discrimination from PABI#2. Note that this listener obtained the best pulse rate DLs of 10-20% at rates around 100 Hz and was poorer at rate discrimination for both higher and lower rates. PABI#2 is the best at speech recognition of all PABI patients, understanding 10-15% of words in sentences.

Gap Detection with Unequal Markers

Traditional psychophysical gap detection does not correlate with speech recognition performance. Gap detection is a measure of temporal processing capability. Typically two identical stimuli are presented in time with either no separation or separated by a short gap in time. Normal hearing listeners can typically detect gap durations of 3-5 ms. Cochlear implant listeners can also detect small gaps of 1-3 ms in similar stimuli presented electrically (Shannon, 1989c). However, relevant temporal gaps in speech



are of longer duration. For example, the temporal gap that defines the voice onset time (VOT) between a plosive consonant and the voicing of the following vowel is on the order of 15-20 ms. Short VOTs are identified as one consonant and longer VOTs are identified as another consonant. We simulated the temporal sequence of the consonant-vowel sequence by presenting a short (20-40 ms) burst of a relatively high frequency pulse train and a longer burst of a low-frequency pulse train simulating a voice fundamental frequency, F0. The two bursts are separated either by no gap in time (standard) or a variable time interval (gap). The detection threshold for the gap was measured as a function of the frequency of the second (vowel-like) burst. The results are presented in Figure 9 for two PABI listeners (top panels) and two ABI non-tumor patients from Verona (lower two panels). Open symbols represent measures from surface ABI electrodes and filled symbols represent data from penetrating electrodes. The dashed line in each figure shows the time interval that corresponds to one period of the F0 frequency. At this gap value there is an inherent ambiguity as to whether there is no gap or a gap of one period of the F0 frequency. Note that many of the functions parallel this line, indicating that the gap detection threshold in this complex stimulus is limited

by the period of the vowel-like stimulus (possibly including an additional fixed time interval). However there is not clear that there is any significant difference in gap detection between PABI and ABI patients, between surface and penetrating electrodes, or between patients with excellent speech understanding (lower two panels) and patients with poor speech understanding (top two panels). Note that the gap detection threshold for these stimuli is on the order of 15-20 ms for F0 frequencies of 100-150Hz, a normal range of voicing fundamental frequencies. Thus, it appears that the categorical distinction between two consonants that differ in VOT may be due to a basic psychophysical phenomenon - the gap between the plosive release and the initiation of voicing is either heard or not heard.

Trigeminal Nerve Activation in PABI#6 and #7

One of the critical issues addressed in the last quarter is that of nonauditory stimulation of the spinal root of the trigeminal nerve in PABI#6 and #7. We observed painful sensations in the ipsilateral face in both of these patients when stimulating with a 250Hz pulse train with an amplitude of less than 1 nC. This amplitude is so small it should not be activating neurons more than 100 microns from the electrode tip and the standard anatomy suggests that the spinal root of the trigeminal is several mm away from the desired electrode location. The fact that other penetrating electrodes produced auditory sensation without side effects in PABI#6 indicated that the penetrating electrode array was in the desired location in the CN. Thus, there was some concern that the device was producing more than the 1 nC of current specified.

To test the implanted hardware Cochlear Corp has a dedicated computer system that can check the integrity of the implanted device and its output. The device is programmed to output a specific current waveform and the electrical signal is recorded at the patient's earlobes. Because the head is largely resistive, the actual electrical voltage signal, attenuated by distance, can be measured at the ear lobes. We were particularly concerned about potential charge imbalances in the biphasic pulses or larger than anticipated current outputs. We first "calibrated" the system on PABI#2, whose penetrating electrodes produced useable auditory sensation. Electrode impedances were measured and the stimulating waveform was measured as a function of the electrode stimulated, the pulse phase duration, and pulse amplitude. All measures appeared normal and regular, i.e. the voltage measured doubled when the specified current was doubled and the biphasic pulses had the correct shape and charge balance.

Next the system was applied to PABI#6 and #7 on July 28. The test stimulus was a single biphasic pulse of 100 us/phase at a current level of 15 uA, resulting in a 1.5 nC pulse. When this pulse was applied to all surface electrodes and penetrating electrodes it produced normal electrode impedance measures, normal charge-balanced stimulating biphasic pulse waveforms, and normal amplitude response. When the stimulus was applied to the electrodes that produced unpleasant activation of the trigeminal nerve the patient reported no sensation. When the stimulus was increased to two pulses separated by 50 ms patient reported a vibration sensation at the back of the neck. When the stimulation was increased to 4 pulses separated by 50 ms each the sensation magnitude increased to the point where it was starting to become uncomfortable. We stopped the stimulation at that point for PABI#6. Similar measures verified proper device function on PABI#7, but the electrodes activating non-auditory sensations were not attempted due to the emotional state of the patient.

In sum, the devices appeared to be working properly on both patients. Electrode impedances were in the range expected, biphasic pulse amplitudes were correct and pulses were properly charge balanced. Our conclusion is that the penetrating electrodes of the PABI device must be reaching the region of the spinal root of the trigeminal nerve. The low activation levels we observed result from physical proximity as well as to a high degree of cross-pulse integration. In electrical stimulation of most auditory structures, we observe little or

no integration across successive stimulation pulses. The time constant of integration across pulses appears to be about 2-3 ms for cochlear implants and possibly 10 times shorter than that for ABI stimulation. In contrast the integration for stimulation of the spinal root of the trigeminal nerve appears to have an integration time constant of more than 50 ms. In our initial activation of the device we typically stimulate each electrode with 250 pps burst of pulses that lasts for 300 ms. While a stimulus of this type may not even be detectable in terms of hearing, the long integration time of the trigeminal nerve causes this stimulus to be strongly activating, even when the individual pulses are each less than 1 nC.

To guard against future non-auditory side effects we will use extreme caution in the initial stimulation of penetrating PABI electrodes. We will initiate the stimulation with single pulses at the lowest output level of the stimulator. We will slowly increase the number of pulses and the pulse amplitude until we elicit a non-auditory sensation (presumably mild because of the cautious approach) or auditory sensations.

Work in the Next Quarter

PABI#8 and #9 are scheduled for initial stimulation in the last quarter of 2006 and PABI#6 is scheduled for a return visit.

Presentations

Shannon RV, McCreery D, Otto SR, Brackmann DE, Hitselberger WE (2006). "The Penetrating-electrode Auditory Brainstem Implant (PABI)", *Neural Interfaces Workshop*, Bethesda, August 23. (podium)

Shannon RV, Otto SR, Brackmann DE, Hitselberger WE, Colletti V (2006). "The Auditory Brainstem Implant: Past, Present and Future", *International Workshop on Neurofibromatosis Type 2: State of the Art*, Paris, Sept 7-9.

Shannon RV, McCreery D, Otto SR, Brackmann DE, Hitselberger WE (2006). "The Penetrating-electrode Auditory Brainstem Implant (PABI)", *International Workshop on Neurofibromatosis Type 2: State of the Art*, Paris, Sept 7-9.

Shannon RV (2006). "Restoration of hearing by electrical stimulation of the human cochlea, auditory brainstem and midbrain", *Medical University of Hanover*, Hanover, Germany, Sept 15.

Shannon RV (2006). "Restoration of hearing by electrical stimulation of the human cochlea, auditory brainstem and midbrain", *2006 Beijing International Symposium of Otolaryngology*, Beijing, Sept 25-26.

Nucleus Auditory Brainstem Implant System Conference and Practicum for Surgeons, Neurosurgeons, and Audiologists, Los Angeles, July 21-22. NOTE: all HEI and HEC ABI/PABI researchers and clinicians participated in an ABI training course. More than 60 attendees were trained in ABI clinical application, including temporal bone drilling, audiological workshop and electrophysiological workshop over the course of two days.

References

Shannon, R.V. (1985). Threshold and loudness functions for pulsatile stimulation of cochlear implants, *Hearing Research*, 18, 135-143.

Shannon, R.V. (1989a). Threshold functions for electrical stimulation of the human cochlear nucleus, *Hearing Research*, 40, 173-178.

Shannon, R.V. (1989b). A model of threshold for pulsatile electrical stimulation of cochlear implants, *Hearing Research*, 40, 197-204.

Shannon, R.V. (1989c). Detection of gaps in sinusoids and pulse trains by patients with cochlear implants, *J. Acoust. Soc. Amer.*, 85, 2587-2592.

Zeng, F.-G., Galvin, J., and Zhang, C.-Y. (1998). Encoding loudness by electric stimulation of the auditory nerve, *NeuroReport*, 9(8), 1845-1848.